Growth process of Ge on Si(100)-(2×1) in atomic-layer epitaxy from Ge_2H_6

Kuang-Hsin Huang, Tsai-Shian Ku, and Deng-Sung Lin
Institute of Physics, National Chiao-Tung University, 75 Bo-Ai Street, Hsinchu, Taiwan
(Received 21 October 1996)

This study investigates the growth process of Ge on Si(100) during atomic-layer epitaxy (ALE) utilizing digermane. The surface ordering, morphology, and stoichiometry of the digermane saturated Si(100) surface at temperatures between 300 and 900 K, as well as the grown films are examined both by scanning tunneling microscopy (STM) and high-resolution core-level photoemission spectroscopy employing synchrotron radiation. An exposure of more than 15 L (1 L=10^{-6} T s) of digermane on the Si(100)-(2×1) surface at room-temperature results in a saturated and disordered surface. When the digermane saturated surface is heated to 725 K for 60 s, diluted Ge dimer chains are created and surrounded by SiH species. Further annealing to 810 K completely desorbs hydrogen from the surface, leaving large two-dimensional islands covering ~41% of its area. The surface recovers its smooth 2×1 structure, but is interspersed with poorly ordered short dimer vacancy lines at 900 K with no observable contrast on the atomic terraces, indicating displacive adsorption of Ge on the terraces. Significant differences of the surface diffusion phenomena between the gas-phase and solid-phase molecular-beam epitaxy (MBE) are observed. Multilayer Si deposition is performed by ALE, i.e., cyclic digermane adsorption at near room temperature, followed by thermal annealing at 900 K. STM images reveal the formation of $2\times n$ structures and increasing roughening of the surface as the growth cycle increases, similar to what occurs during MBE. Issues related to the atomic origins of surface core-level shifts and the chemical composition of the surface layer resulting from the formation of mixed Ge-Si or Ge-Ge during the submonolayer adsorption of Ge on Si(100) are also discussed. [S0163-1829(97)05832-3]

I. INTRODUCTION

Surface processes during chemical vapor deposition (CVD) and the atomic-layer epitaxy (ALE) of group-IV elements currently have received extensive interest.[1–8] As the trend toward reducing device dimensions continues, submicrometer Si technology places increasingly stringent demands on thin-film techniques. One of the most significant developments has been the introduction of ALE. This cyclic vapor-phase epitaxial film growth technique incorporates self-limiting kinetic processes which result in the deposition of quantized thickness per growth cycle. Because its deposition rate is kinetically self-limiting, ALE has proven itself a highly effective technique for improving crystalline quality and layer thickness uniformity.[1,9] Its cyclic deposition process facilitates the growth of materials with extremely narrow single or alternative doping spikes for quantum-layer devices.

An example is Si ALE on Si(100)-(2×1) with disilane as the gas source.[1] On exposure to more than 10 L of disilane, the Si(100)-(2×1) surface adsorbs a nominal 0.5 ML (1 ML=6.78×10^{14} cm^{-2}) of dissociated fragments (SiH_3 trihydride and SiH_2 dihydride) at <400 K. Since the hydrides saturate all the surface dangling bonds, the sticking probability of any excess disilane is essentially zero, the Si(100) surface is passive to further disilane exposure, and the disilane flow is then halted. Once the surface is heated to a high temperature or irradiated with UV laser pulses to desorb H, the net deposition is ~0.5 ML. Repeating this growth cycle, first saturating the Si(100) surface with disilane, followed by high-temperature annealing, results in a quantized (0.5 ML layer per cycle) deposition of Si. Because the surface, rather than the supply of gas source, controls the growth via the self-limiting process, only a single layer or less is deposited in each cycle which can result in low defect density and satisfactory layer thickness uniformity.

This study reports the findings of an investigation conducted by a combination of scanning tunneling microscopy (STM) and synchrotron core-level photoemission into Ge ALE on Si(100)-(2×1) utilizing digermane. Chemically similar to Si_2H_6 (disilane), Ge_2H_6 (digermane) functions as excellent precursor molecules for Ge growth.[4,7] It exhibits high sticking probability (~0.5) on Si and Ge surfaces and its lower decomposition activation energy for both gas phases and surface reactions allows a lower deposition temperature. The heteroexpitaxy of Si and Ge on each other is of relevance both to fundamental thin-film science and to the potential applications of $Si_{1-x}Ge_x$ heterostructures and Si/$Si_{1-x}Ge_x$ strained-layer superlattices in optoelectronic devices.[10,11] The apparently simple Si/Ge growth systems involve two group-IV semiconductor materials of similar physical and chemical properties, yet give rise to a variety of interesting phenomena. The early stages of Ge film growth on Si has long continued to be of considerable interest as a classic Stranski-Krastanov system exhibiting pseudomorphic layer-by-layer growth up to ~3-ML coverage followed by three-dimensional island formation.[12–16] Although the surface morphology, atomic structure, and surface stress of Ge-covered Si(100) have been thoroughly examined, previous studies resting on solid-phase molecular-beam epitaxy (MBE) have revealed discrepancies in the details of the atomistics of the growth, especially in the submonolayer regions.[17] This work provides challenging comparisons between Ge ALE growth on Si(100) and the corresponding MBE process.

The techniques applied herein include core-level photo-

 © 1997 The American Physical Society

emission spectroscopy utilizing synchrotron radiation and scanning tunneling microscopy. Complementary in nature, they allow surface chemical analysis and real-space imaging of the atomic structure and morphology to be performed. STM images reveal that at room temperature the digermane-saturated surface is highly disordered. The overlayer exhibits increased ordering with, by heating to 725 K, a larger fraction of the admolecules in one-dimensional trains, and by 810 K, the STM micrographs indicate that essentially almost all of the admolecules are captured in well-defined 2×1 two-dimensional islands, covering ~41% of the surface. Multilayer growth was examined, following the standard procedure of ALE. The Si surface is first saturated with digermane at near room temperature, and then annealed to high temperatures to desorb hydrogen, giving a net deposition of around 0.5 ML of Ge atoms. This quantized deposition process is repeated. The findings confirmed that the morphology and atomic structures of the resulting Ge films in Si(100) via ALE closely resemble those pertaining to growth obtained by MBE, even though the presence of terminating hydrogen on the surface during CVD growth gives rise to different surface reactions. Finally, we discuss issues concerning the formation of Ge-Ge or mixed Ge-Si dimers during submonolayer growth of Ge on Si(100)-(2×1) in light of the high-resolution core-level photoemission spectroscopy.

II. EXPERIMENTAL PROCEDURE

STM measurements were performed in a stainless-steel chamber equipped with a bolt-on commercial UHV-STM system(Omicron). The chamber has a base pressure less than 1×10^{-10} torr. The tips of the STM were electrochemically etched tungsten wires. All images were obtained in a constant current mode with a tunneling current of ~0.3 nA. Slight distortions due to thermal drift were not corrected.

The photoemission experiments were carried out in a separated μ-metal UHV system utilizing synchrotron radiation from a 1.3-GeV storage ring at the Synchrotron Radiation Research Center in Hsinchu, Taiwan. Light from the storage ring was dispersed by a 6-m low-energy spherical grating monochromator. All the Ge_2H_6 adsorption, annealing, and Ge-film growth were prepared *in situ* in UHV conditions. Photoelectrons were collected and analyzed by a large hemispherical analyzer. The overall energy resolution was less than 120 meV.

The Si(100) samples were sliced from B-doped wafers with an electrical resistivity of around 10 Ω cm, corresponding to a dopant concentration of approximately 1.5×10^{15} cm^{-3}. The wafer's misalignment is around 0.1° toward ⟨011⟩. Substrate cleaning involved outgassing at ~900 K for 10 h followed by dc heating to ~1450 K for a few seconds. Digermane (Voltaix, ultrahigh purity grade, 20% in He) was introduced into the chamber through a precision leak valve. The dosing pressure, in the 10^{-7}-torr range, was monitored by an ionization gauge which did not directly face the sample. The pressure readings of the ion gauge were corrected by the gauge's sensitivity to He and Ge_2H_6, which are around 0.18 and 2.4, respectively, relative to air.[8] The sample was annealed by passing a current through it an its temperature was measured with an infrared pyrometer. Each annealing lasted for 60 s.

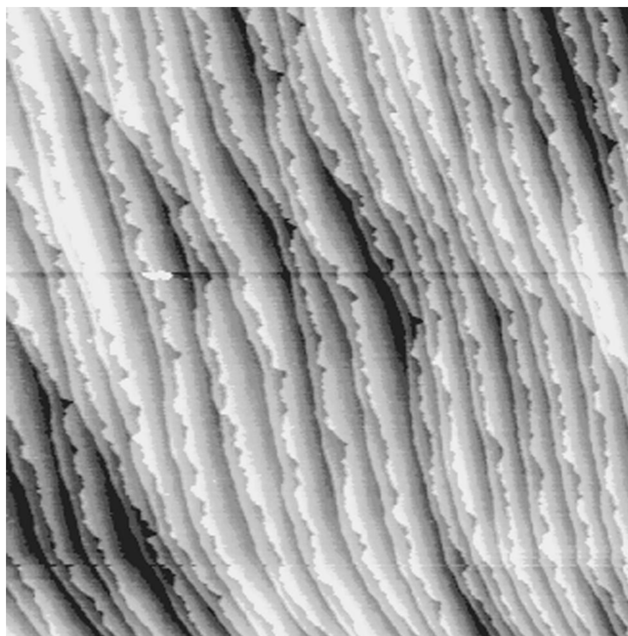

FIG. 1. STM image of a clean Si(100)-(2×1) surface. The scan range is $30\,000\times30\,000$ Å^2.

III. RESULTS AND DISCUSSION

A. Thermal annealing of the first growth cycle

A clean Si(100) surface is known to exhibit a 2×1 reconstruction. Surface atoms form dimer rows to lower the surface energy by eliminating one of their two dangling bonds. Figure 1 depicts a $30\,000\times30\,000$-Å^2 STM image of the initially clean Si(100)-(2×1) surface. At this scale, individual atoms and dimers cannot be seen and the main feature are monoatomic steps. This image confirms the earlier finding concerning the Si(100)-(2×1) step structure.[18] The steps are alternatively smoother and rougher; they correspond to the so-called S_A and S_B steps, respectively. Each step separates two degenerate reconstruction domains [2×1 and 1×2 domains] with dimer rows perpendicular to each other. The 2×1 [1×2] domains are the terraces with their dimer rows running perpendicular (parallel) to the domain edges.

Exposing clean Si(100)-(2×1) to digermane at room temperature results in randomly distributed dissociated fragments on the surface, which exhibits no correlation between Ge_2H_6 adsorption and local defects or steps. Figure 2(a) indicates that the fully saturated surface with 15-L digermane was highly disordered. The digermane-saturated adlayer comprises a mixture of GeH_2, GeH, SiH, and some residual GeH_3, and multiple internal reflection infrared spectroscopy and photoemission studies revealed.[4,7] A previous ultraviolet photoemission spectroscopy study indicated that the exposure of digermane of Si(100)-(2×1) resulted in molecular adsorption below 100 K, but generated a surface covered with GeH_3 radicals, stable between 110 and 150 K.[5] Hence, at room temperature, most GeH_3 radicals further decompose to GeH_2(ad) and H(ad), which process breaks a dimer bond by inserting H and leaves a saturated GeH_2 radical in a 1×1 surface site. Therefore, the disordered digermane-saturated surface displayed in Fig. 2(a) indicates that the GeH_2 fragments on the surface are not sufficiently mobile to form islands or clusters.

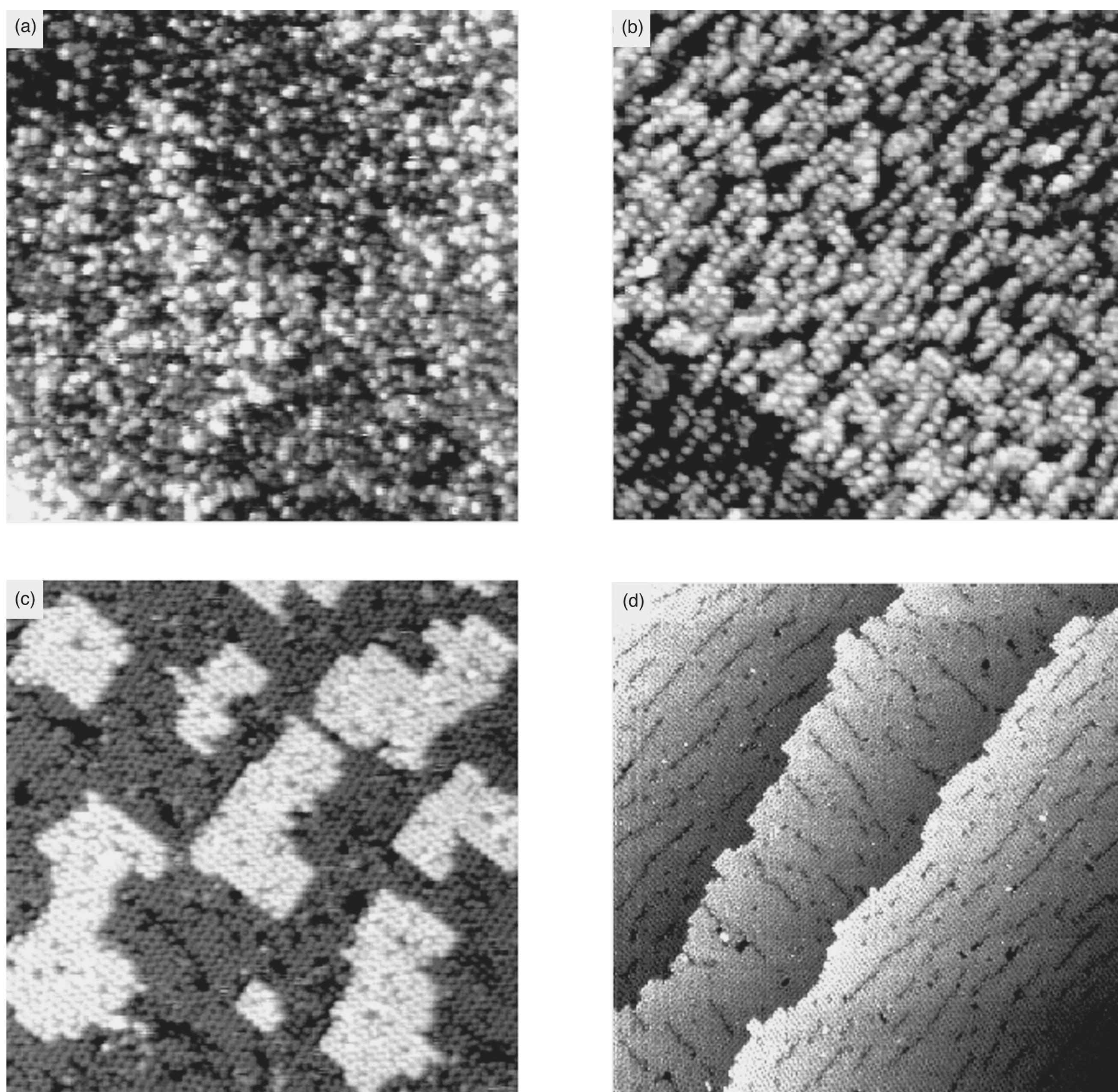

FIG. 2. STM images of (a) Si(100)-(2×1) saturated with a 15-L digermane dose at 300 K, and the same surface after annealing to (b) 725, (c) 810 and, (d) 900 K. The scanned areas are 450×450 Å^2 for (a)–(c), and 1000×1000 Å^2 for (d). The sample bias used with −2 V for (a) and (b), and +2 V for (c) and (d). A monoatomic step can be discerned around the lower left corner in (a) and middle left corner in (b).

Subsequent heating of the digermane-saturated Si(100) surface has the effect of thermally decomposing the surface hydrides (GeH_2 and GeH_3) into GeH, liberating all the adsorbed hydrogen and leaving only Ge atoms on the surface. This picture of thermal dissociation processes corresponds to the temperature-programmed desorption of H_2 measurements, which comprises two H_2 desorption maxima α(~600 K) and β_1(~800 K).[5] The two desorption states α and β_1 attributed to H_2 desorption from the decomposition of GeH and SiH, respectively. Figure 2(b) displays a 450×450-Å^2 STM image after annealing at 725 K for the room-temperature saturated surface. The surface in Fig. 2(b) still lacked long-range ordering; however, the majority of the surface admolecules in the filled-state image ordered in lines consisting of a few bright spots. These short linear trains lie in parallel on the same terrace and perpendicular to those on the terrace separated by a single atomic step. Furthermore, the direction of the trains are normal to the smoother S_A atomic steps, which are parallel to the dimer rows. The annealing temperature (725 K) was located between the α (600 K) and β_1 (800 K) desorption peaks in the H_2 thermal-programmed desorption spectra. Therefore, it could be expected that all the H attached to Ge had been driven off, and only Ge atoms and SiH species remained present on the surface. This reaction step was also confirmed by a previous photoemission study.[7] In addition, the atomic chains in Fig. 2(b) appear to closely resemble the ''diluted dimers'' observed as the prevalent adsorbate configuration during the

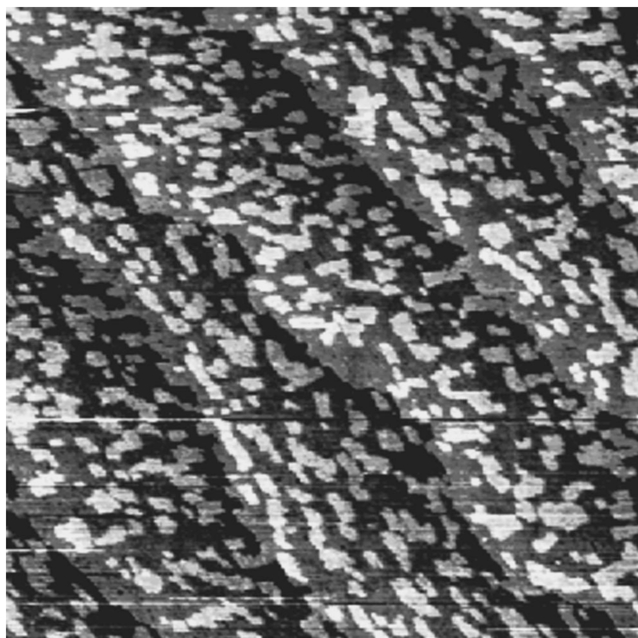

FIG. 3. Large area STM image for the same surface of Fig. 2(c). The area is 3000×3000 $Å^2$.

MBE Si deposition at ~385 K.[19] The ''diluted dimers'' are metastable lines of dimers arranged end to end. Each of the constituent dimers ordered in a line lie in a trough between substrate dimer rows and are perpendicular to them. All the above observations lead to attributing the linear chains in Fig. 2(b) to be Ge ''diluted dimers'' interspersed on the remaining hydrogen terminated Si substrate. At this temperature, Ge ad-dimers obtained from MBE posses sufficient diffusion energy to form large-two dimensional (2D) islands on clean Si(100)-(2×1). The formation of diluted dimers with partial ordering can be attributed to the hindrance of the Ge surface diffusion rate due to the presence of SiH.

Annealing a surface, such as that in Figs. 2(a) or 2(b) to 810 K for 60 s, resulted in the well-ordered surface depicted in Fig. 2(c). The randomly dispersed digermane fragments in Fig. 2(a) were ordered to form 2D, buckled 2×1 islands. The dimer rows, which comprised the islands in Fig. 2(c), are orthogonal to those of the substrate, and are consistent with the formation of a layer of a diamond structure. The substrate dimer rows also exhibited irregular buckling, which might be related to long-range interactions involving the 2D islands and their surroundings. Since the desorption maximum of H_2 from SiH is about 800 K, annealing at 810 K for 60 s is sufficiently high to completely desorb hydrogen atoms from the surface. Therefore, the 2D islands in Fig. 2(c) may be readily attributed to Ge dimers.

On the basis of Fig. 2(c), the saturation coverage of digermane of Si(100) can be estimated at rough 0.37 ML. To obtain a more precise picture of island coverage, Fig. 3 gives an overview image of a scale 3000×3000 $Å^2$ for the same surface area depicted in Fig. 2(c). Notably the islands in Fig. 3 dispersed uniformly on all the terraces, and the 2D islands did not exhibit much anistropy. From Fig. 3, the island coverage may be deduced to be 0.41. Since the Ge atoms incorporated into the step edge cannot be taken into account, this coverage represents a lower bound. Furthermore, the dimerized 2D islands may represent only ~75% of the deposited Ge while, at this temperature, the other ~25% move to the second layer, as indicated by the Ge 3d spectra in Fig. 4(b) (see Sec. III B). The saturation coverage may be estimated nominally as 0.5 ML. which correlates closely with previous experimental results for Si_2H_6 adsorption on Si(100) and Ge(100).[1,3,8] Monte Carlo simulations also revealed that the coverage for Si_2H_6 adsorption on Si(100) was limited to 0.43 ML, based on the similar surface reaction mechanism,[3] on site blocking by H, and on steric hindrance. These findings together with a previous core-level photoemission study of thermal reactions indicates that the overall trends of adsorption mechanism for Ge_2H_6 closely resemble those for Si_2H_6 interaction on Si(100).[8]

Figure 2(d) depicts a well-ordered and relatively smooth surface after further annealing at 900 K. The 2D Ge islands appearing in Fig. 2(c) disappeared entirely. In Fig. 2(d), three terraces separated by two monoatomic steps are observed. Within the domains, many short dark dimer vacancy lines (VL's) are clearly observable. Figure 2(d) indicates that these VL's are all perpendicular to the surround dimer rows and well separated, revealing the strong repulsion between VL's. Although the length of the VL's varies, they are uniformly distributed on the entire surface. If the usual picture of step-flow growth occurred during annealing, the 2D Ge islands in Fig. 3 should simply diffuse and adhere to nearby steps. Once Ge atoms are incorporated into the original steps, remaining intact, the immediate formation of a well-defined 2×n structure [see Fig. 6(a)] in those areas coexists with the remaining clean Si-terminated 2×1 areas. However, the STM image does not reveal any supposed contrast between the Ge-terminated regions and the original, Si-terminated areas, and none was observed on the surfaces of a similar growth system by low-energy electron diffraction and microscopy either.[12] It is thus clear, as proposed by Tromp,[12] that Ge atoms displace Si in the terrace and together form a relatively homogeneous, mixed Ge-Ge and Si-Si dimer surface. It is also notable that all the surface dimers in Fig. 2(d) appeared buckled. By comparison, at room temperature, only certain portions of the dimers on the clean Si(100)-(2×1) were asymmetric.

B. Multilayer growth by atomic-layer epitaxy

As noted above, saturating the Si(100) surface with digermane at room temperature followed by high-temperature annealing yielded a net deposition of around $\frac{1}{2}$ ML of Ge. Repeating the cycle results in a controllable, quantized deposition generally known as atomic-layer epitaxy. In this study, an initial saturation exposure of 15 L and an annealing temperature of 900 K for 60 s where selected. Although Ge deposition at this annealing temperature produces films that are not in their thermodynamical ground state,[17] the temperature is sufficiently high to promote step flow and island incorporation for smooth film growth, as is depicted in Fig. 2(d), while minimizing the possible intermixing between Si and Ge.

Figures 4(a) and 4(b) display photoemission spectra of Si 2p and Ge 3d, respectively, for various numbers of cycles of Ge deposition. The binding energy refers to the bulk component of the Si $2p_{3/2}$ line (see below). The bottom spectrum of Fig. 4(a) represents a surface-sensitive Si 2p spectrum for

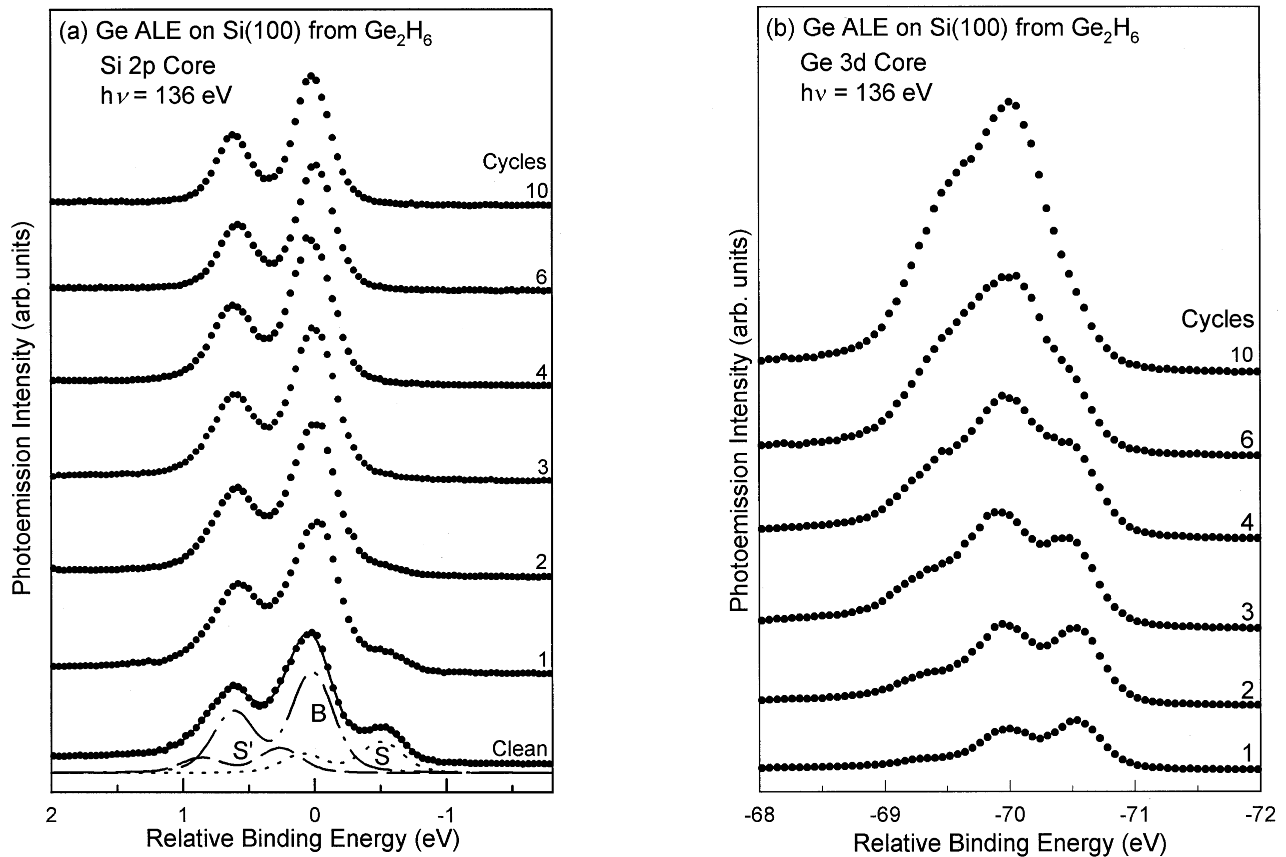

FIG. 4. Photoemission spectra (filled circles) for (a) the Si $2p$ and (b) and Ge $3d$ core levels for various numbers of cycles of ALE growth of GE on Si(100). Each cycle involves an exposure of 15-L digermane at $\sim$325 K followed by annealing at 900 K. The bottom spectrum of (a) is for the clean Si(100)-(2×1) surface. The solid curve is a fit to the spectrum. The curves labeled B, S, and S' are the results of a decomposition into individual components which consist of a pair of spin-orbit split peak. The B component is derived from the bulk; S and S' are surface related. The relative binding energy refers to the Si $2p_{3/2}$ line of the B component.

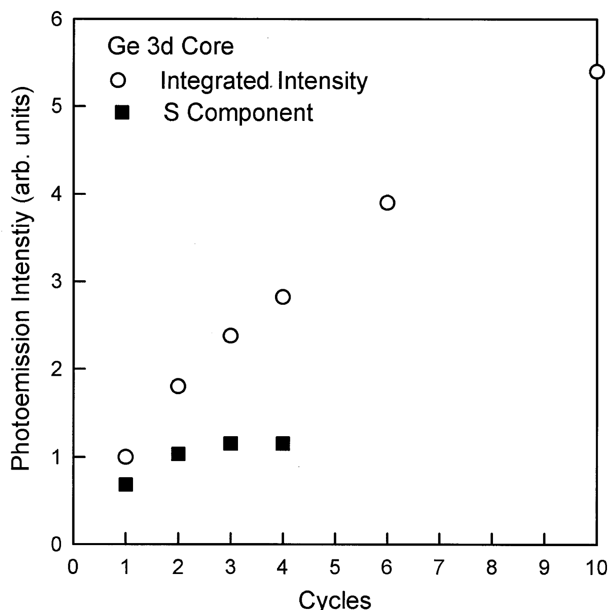

FIG. 5. Integrated photoemission intensity (circles) and photoemission intensity of the S component alone (filled squares) of Ge $3d$ for various cycles of Ge growth on Si(100). Each cycle involves an exposure of 15-L digermane at $\sim$325 K followed by annealing at 900 K.

clean Si(100)-(2×1) and the results of a least-squares analysis. Following standard procedure, the spectrum is analyzed in terms of three spin-orbit-split components S, S', and B of identical line shape, corresponding to signals derived from the dimerized surface layer, the second layer, and the bulk, respectively.[20] The S component is responsible for the well-separated shoulder on the lower-binding-energy side, and its intensity can be deduced by fitting. Upon deposition of Ge by ALE from Ge_2H_6, the intensity of S decreases nearly to zero after two growth cycles, indicating that the surface becomes a Ge layer and the top layer of Si then becomes a second layer. The presence of S' in the Si $2p$ spectrum for the clean Si(100) is shown by the valley between two spin-orbit-split peaks of the B component filling in. The S' component began decreasing slowly and completely disappeared after more than six cycles of Ge growth. The reduction of the S' component can be best understood by examining the changes in the relative depth of the valley between the two spin-orbit peaks. At ten cycles ($\sim$5 ML coverage) of Ge growth, the line shape of the top spectrum in Fig. 4(a) consists of only two spin-orbit peaks, reflecting the bulk emission. This is because the bonding between Si and Ge closely resembles that of Si and Si, and, as a result, all Si atoms under such a thick layer of Ge are in a bulklike bonding environment.

The line shapes of the Ge $3d$ for the bottom three spectra in Fig. 4(b) can be decomposed into a few components. The

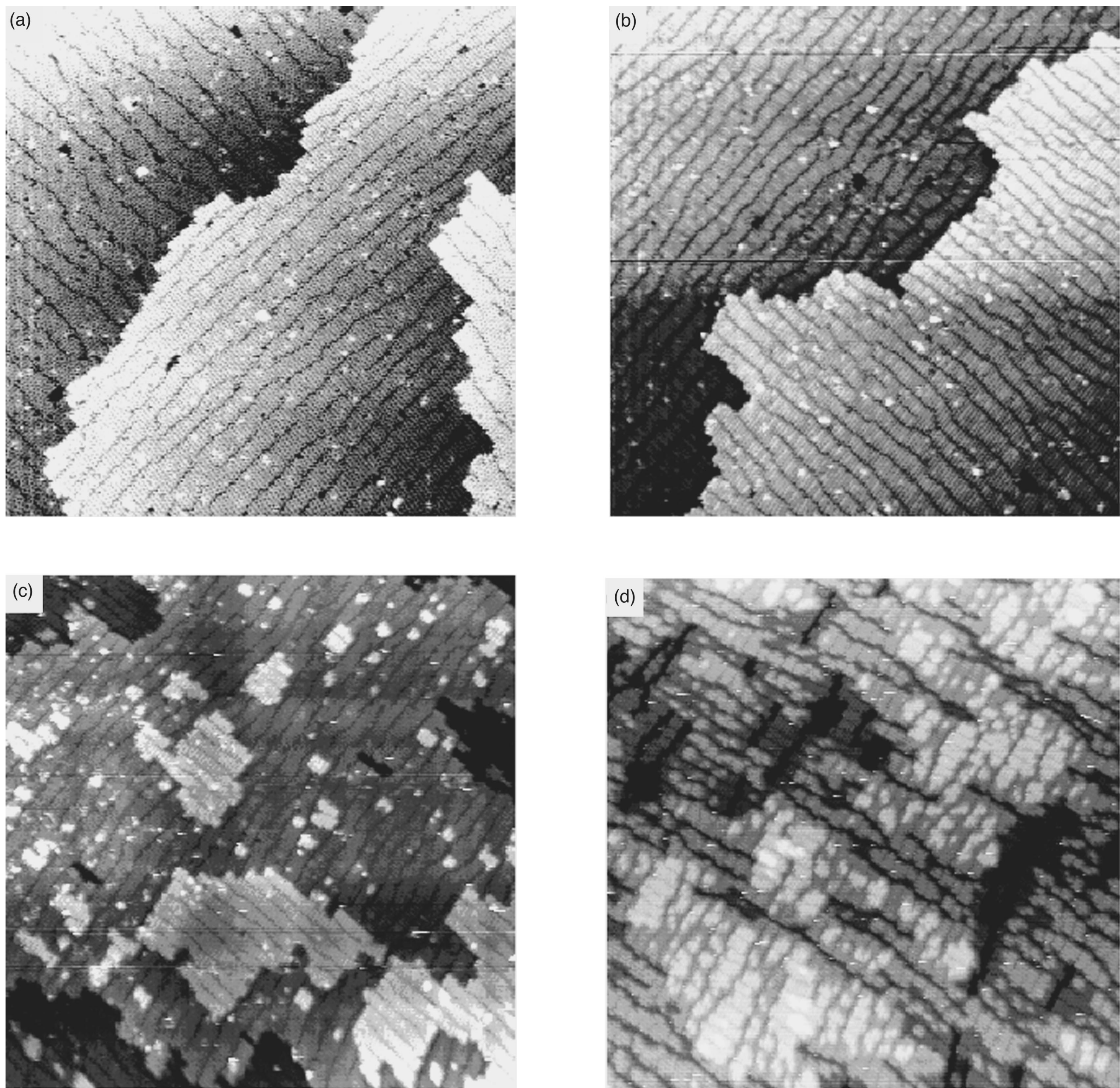

FIG. 6. 1000×1000-Å^2 STM images of Si(100) after (a) two, (b) six, (c) nine, and (d) 15 cycles of ALE growth of Ge. Each cycle involves an exposure of 15-L digermane at ~325 K followed by annealing at 900 K.

implications are discussed in Sec. III C. The broadening and loss of characteristic features in Ge $3d$ line shapes for six and ten cycles can be attributed to the gradually increasing surface roughness and disorder. The integrated intensity of Ge $3d$ as a function of growth cycles is plotted in Fig. 5. The net Ge deposition in each cycle is expected to be about the same due to the chemical similarity of Ge and Si dimers. However, the indiffusion of partial Ge population into deeper layers (see Sec. III C) reduce the integrated intensity of Ge $3d$ due to a short electron mean free path, leading to slight deviation of the data points in Fig. 5 from a linear incline. The overall trends of these Si $2p$ and Ge $3d$ spectra in Figs. 4(a) and 4(b) closely correlate with those found during MBE growth of Ge, and the calibration of the Ge coverages should be more satisfactory here since ALE was employed.

Figures 6(a), 6(b), 6(c), and 6(d) depict the surface after two, six, nine, and 15 cycles of Ge growth of Si(100), respectively. In Fig. 6(a), the $2\times n$ (on an average, $n\sim12$) reconstruction, signaled by the dark VL's, is clearly observable. The VL's extend for hundreds of Å but the ordering of the $2\times n$ structure is poor in that the distance between two VL's exhibits a very broad distribution. As the Ge coverage increases to ~3 ML, the VL's concentration also increases, as Fig. 6(b) illustrates. This figure basically depicts the same $2\times n$ reconstruction as Fig. 6(a), but the VL's concentration increases (on an average, $n\sim8$) and the degree of $2\times n$ ordering appears better in that the distribution of n is sharper. These observations were fairly consistent with previous STM studies of Ge-covered Si(100) utilizing MBE for corresponding coverages.[18] The formation of a $2\times n$ structure and its degree of ordering has been associated with stress changes on the Ge-covered Si(100). Since there are no trenches in the

second layer at the locations of the VL's of the first layer in Fig. 6(b), the dimer vacancies must have been filled. Upon completing nine cycles (~4.5 ML) of Ge ALE growth, multilayer growth had started, as Fig. 6(c) indicates. Augmenting ALE growth cycles results in increased surface roughness, as illustrated in Fig. 6(d). Figure 6(d) basically depicts a multilayer surface, each layer consisting of many small $2\times n$ domains bounded by VL's of the same layer and trenches, which are extensions of those VL's on deeper layers. These measurements were consistent with previous reports which confirmed that the Ge growth on Si(100) is layer by layer, up to a thickness of ~3 ML with the surface maintaining a nominal 2×1 structure.[13–16]

C. Chemical composition of the dimer layer

In the above sections, interpreting the data was based on a theoretical calculation which revealed that Ge possesses a lower surface energy, and that a full layer of Ge covers the surface of a $Ge_{0.5}Si_{0.5}(100)$ alloy.[21] Full Ge termination upon the adsorption of Ge on Si(100) at 1 ML or above of coverage was also clearly suggested both by theoretical calculations[17] and many experimental studies employing low-energy electron microscopy,[12] low-energy electron diffraction,[13], STM,[13–15] and ultrahigh vacuum transmission microscopy.[16] As Ge is deposited on Si(100), however, a surface layer consisting of a mixture of Si-Ge dimers is speculated to form beneath a 1-ML coverage.[22] Distinguishing between Si-Si, Ge-Ge, and Si-Ge dimers is a problem, because Si and Ge are extremely similar to their atomic, electronic, and chemical properties. Therefore, the atomistic process of Ge incorporation and the compositional distribution of the surface and subsurface regions all remain unclear, despite extensive studies.

These questions concerning the initial stages of growth are also attended by problematic interpretations of the atomic origins of surface-shifted core levels in the photoemission spectra for the clean Si(100)-(2×1) and Ge on Si(100) (2×1).[20,22–26] In Sec. III B, the peak assignment for the S components in the Si $2p$ spectrum for clean Si(100) in Fig. 4(a) is one complete monolayer of dimerized Si atoms on the surface, including both up and down dimer atoms in the asymmetric dimer model. An alternative interpretation is to attribute the S component to up dimer atoms only (one-half of a monolayer). These differing interpretations may be referred to as the full-layer and half-layer interpretations, respectively. In two previous photoemission studies of MBE growth of Ge on Si(100), similar results for Si $2p$ and Ge $3d$ core-level spectra were variously attributed to the different thicknesses of calibration of film growth in the submonolayer region.[20,22] For example, the intensity of the S component, which is a quantitative measure of the surface area that remains clean, decreased to zero at ~0.5 ML in Ref. 22 but at ~1 ML in Ref. 20. The authors of Ref. 22 thus concluded that Ge initially grows as asymmetrically mixed Ge-Si dimers, with Ge occupying the up atoms since their emission from the up Si atoms (the S component) disappears at a 0.5-ML coverage. On the other hand, the authors of Ref. 20 referred to the 1-ML interpretation, based on assuming pure Ge-Ge dimer growth for the first monolayer, and on the fact that the S component is eliminated at a ~1-ML Ge coverage.

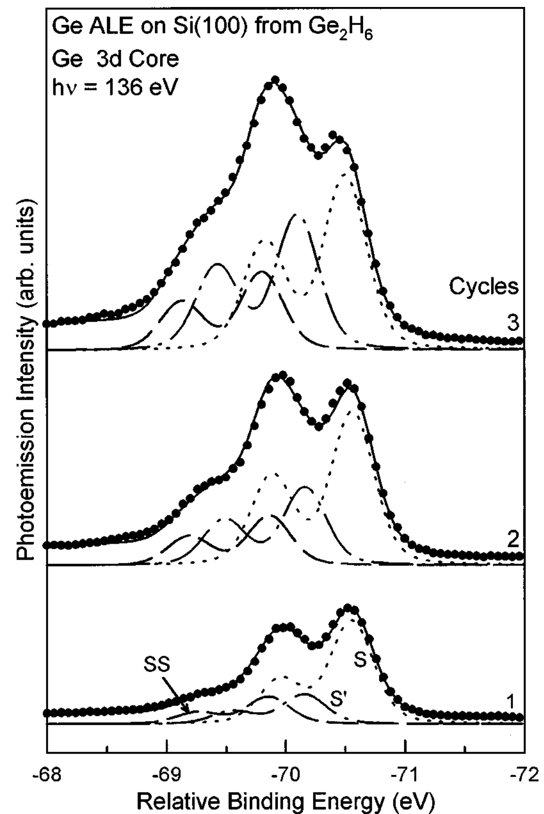

FIG. 7. The decomposition of the Ge $3d$ spectra [taken from Fig. 4(b)] into three curves (S, SS, and S') for the first three cycles of ALE growth of Ge on Si(100). The solid curves are overall fit to the spectra. Details of the peak assignments are given in the text.

As indicated in Sec. III B, the atomic-layer epitaxial growth of Ge from Ge_2H_6 offers quantized deposition and, therefore, should provide a self-calibrated thickness measurement. In Fig. 4(a), the intensity ratio of S/B decreased ~70% from 0.275 for clean Si(100)-(2×1) to ~0.09 for one cycle of growth and ~95% for two cycles. Assuming that the saturation coverage of 0.5 ML is accurate, the coverage determinations in Ref. 20 are higher than, and those in Ref. 22 lower than, the actual values.

Figure 7 displays Ge $3d$ core-level spectra taken from Fig. 4(b) for the first three cycles of Ge growth and the results of decomposition. Note that the Ge $3d$ spectrum taken from clean Ge(100)-(2×1) in Ref. 8 shows a line shape closely resembling that of Si $2p$ for Si(100)-(2×1) due to the similarity of the two surfaces. There are again three major components, B, S', and S, where the S component, shifted to lower binding energies, can be associated with the dimers on the surface. For a more relevant comparison with the spectra in Ref. 22, the line shapes in Fig. 7 are described as the combination of three components S, SS, and S' accordingly. The authors of Ref. 22 assigned peaks S, SS, and S' to the up atoms of mixed Ge-Si dimers, the down atoms of pure Ge-Ge dimers, and Ge in deeper layers, even though most theoretical and experimental studies have indicated that the interface between the grown Ge film and Si(100) substrate is abrupt.[12–15,27] In an attempt to analyze the absolute atomic population of the S component in Ge $3d$ spectra, the relative emission intensity of the S component

for the first four growth cycles was measured by monitoring the photocurrent from a gold mesh, the results of which procedure are plotted in Fig. 5. After the first growth cycle, the intensity of the S component accounts for 70–80 % of the total Ge $3d$ emission (depending on using two or three components in the fitting), or ~0.4-ML Ge atoms, assuming that the total amount of Ge is 0.5 ML. The S intensity increased by around 50%, 70%, and 70% after two, three, and four growth cycles, respectively. Attempting to deduce the intensity for higher growth cycles yielding values close to that of the fourth growth cycle. However, the uncertainty is considerable, since the line shapes are broad and do not easily afford satisfactory fits. The calculated population of the S component is, therefore, ~0.65 ML at the end of four growth cycles. The number of dimer vacancies on the corresponding Ge-covered Si(100) surface is ~13%. Moreover, the core-level emission from the Ge dimers on two sides of the dimer vacancies can easily contribute to the S' or SS peaks due to the charge transfer upon rebonding the second-layer atoms underneath the dimer vacancies.[28] These populations together sum up to ~1 ML. This finding is also consistent with theoretical studies which have revealed that the surface of Ge-covered Si(100) is terminated completely by Ge above 1-ML coverage.[17] Because the energy associated with surface strain is only a fraction of an meV/atom,[17] which is far smaller than the typical energies encountered in the kinetic processes, it is unlikely that the mixed Ge-Si dimers would become an energy ground state if and only if the Ge coverage is less than 1 ML.

If the 2D islands in Fig. 2(c) consist mainly of Ge-Si mixed dimers and thus incorporate only ~0.2 ML of the Ge populations, the surrounding substrate areas must contain the rest of Ge (0.2–0.3 ML) occupying the up atom positions. The scenario of the atomistic process of forming the surface of Fig. 2(c), in such a case, is that about half of the Ge population displaces Si from the substrate to form Ge-Si dimers, and the expelled Si diffuse and form mixed Ge-Si islands with the other half of the Ge. If this picture describes the growth of the first cycles accurately, the atomic arrangements for Ge in Figs. 2(c) and 2(d) and their associated Si-Ge misfit strains are essentially the same, despite the different morphology of the two surfaces, since the line shapes for Si $2p$ and Ge $3d$ spectra remain largely unchanged at annealing temperatures above 810 K. However, no dimer vacancy lines such as those appearing in Fig. 2(d) can be observed in Fig. 2(c).

The above considerations suggest that the pure Ge dimers are stable species during the deposition of Ge/Si(100). The conclusion that Ge predominantly grows as mixed Ge-Si dimers up to 0.8 ML by Pattey *et al.* was solely drawn based on the thickness determinations, which could also be problematic.[22] The deposition of 0.5-ML Si atoms on Ge(100)-(2×1) using disilane is a very similar, although not identical, system for comparison.[8] A previous photoemission study of this system showed that the intensity of the Si $2p$ core level drops by more than 70% after the desorption of H. If the Si atoms merely moved into the down dimer positions, there would be little reduction, but the intensity reduction is too large for all these Si atoms to reside in the layer just below the dimer layer. Most of them must have moved into deeper layers, and the composition of the upper most atomic layer consists of nearly 100% Ge. This phenomena clearly indicates that the Ge-Ge dimers are energetically more favorable than Ge-Si dimers. However, the surface composition of the Ge/Si(100) systems is not likely to be in the idealized states with 100% pure Ge-Ge dimers. Since the entropy factor is important at a high temperature, randomly mixed states consisting of both Ge-Ge and Ge-Si dimers become more favored, as illustrated in Ref. 21.

IV. SUMMARY

Combining microscopy (STM) and spectroscopy (core-level photoemission) techniques provided detailed infomation about the growth process and the consequent surface structure of Ge ALE on Si(100)-(2×1) employing digermane. At room temperature, the adlayer on Ge_2H_6-saturated Si(100)-(2×1) appeared to be completely disordered. When the digermane-saturated surface was heated to 725 K for 1 min, the formation of partially ordered diluted Ge dimer chains was observed. The surface was interspersed with large 2D islands covering ~41% of its area. No denuded zone was present on the surface, in contrast to that during MBE. At 900 K, the surface-recovered 2×1 dimer rows interrupted by poorly ordered short dimer vacancy lines with no observable contrast on the atomic terraces. Multilayer Si deposition was performed by ALE, i.e., cyclic digermane adsorption at near room temperature followed by thermal annealing at 900 K. Overall, the trends observed for multilayer Ge deposition in the present ALE experiments were similar to those for MBE Ge thin-film growth. The chemical composition of the surface layer resulting from mixed Ge-Si or Ge-Ge forming during submonolayer adsorption of Ge on Si(100) was discussed.

ACKNOWLEDGMENTS

The authors wish to thank the National Science Council, Republic of China in Taiwan, for financially supporting this work under Contract Nos. NSC86-2613-M009-001 and NSC85-2112-M009-024. The authors are also grateful to T.-W. Pi for loaning us the photoemission chamber, to T.-C. Chiang for discussions, and to P. Wagner of Wacker Siltronic for providing samples.

[1] D. Lubben, R. Tsu, T. R. Bramblett, and J. E. Greene, J. Vac. Sci. Technol. A **9**, 3003 (1991), and references therein.

[2] S. M. Gates, Surf. Sci. **195**, 307 (1988); R. Imbihl, J. E. Demuth, S. M. Gates, and B. A. Scott, Phys. Rev. B **39**, 5222 (1989).

[3] J. J. Boland, Phys. Rev. B **44**, 1383 (1991).

[4] B. M. Ning and J. E. Crowell, Appl. Phys. Lett. **60**, 2914 (1992); Surf. Sci. **295**, 79 (1993).

[5] D.-A. Klug, W. Du, and C. M. Greenlief, J. Vac. Sci. Technol. A **11**, 2067 (1993); Chem. Phys. Lett. **67**, 2187 (1991).

[6] M. J. Bronikowski, Y.-W. Wang, M. T. McEllistrem, D. Chen,

and R. J. Hamers, Surf. Sci. **298**, 50 (1993).

[7] D.-S. Lin, K.-H. Huang, T.-W. Pi, and R.-T. Wu, Phys. Rev. B **54**, 16 958 (1996).

[8] D.-S. Lin, T. Miller, and T.-C. Chiang, Phys. Rev. B **47**, 6543 (1993).

[9] J. M. Heitzinger, J. M. White, and J. G. Ekerdt, Surf. Sci. **299**, 892 (1994), and references therein.

[10] H. Temkin, J. C. Bean, T. P. Pearsall, N. A. Olson, and D. V. Lang, Appl. Phys. Lett. **46**, 155 (1986).

[11] R. A. Soreff, Proc. IEEE **81**, 1687 (1993).

[12] R. A. Tromp and M. C. Reuter, Phys. Rev. Lett. **68**, 954 (1992); R. A. Tromp, Phys. Rev. B **47**, 7125 (1993).

[13] U. Kökler, O. Juska, B. Müller, M. Horn-von Hoegen, and M. Pook, Ultramicroscopy **42-44**, 832 (1992); F. Iwawaki, M. Tomitori, and O. Nishikawa, *ibid.* **42-44**, 902 (1992).

[14] Y.-M. Mo and M. G. Lagally, J. Cryst. Growth **11**, 876 (1991).

[15] T. Nakayami, Y. Tanishiro, and K. Takayanagi, Surf. Sci. **273**, 9 (1992).

[16] M. Hammer, F. K. Legoues, J. Tersoff, M. C. Reuter, and R. M. Tromp, Surf. Sci. **349**, 129 (1996).

[17] F. Liu and M. G. Lagally, Phys. Rev. Lett. **76**, 3156 (1996), and references therein.

[18] F. Wu, X. Chen, Z. Zhang, and M. G. Lagally, Phys. Rev. Lett. **74**, 564 (1995), and references therein.

[19] P. J. Bedrossian, Phys. Rev. Lett. **74**, 3648 (1995); A. van Dam, J. van Wingerden, M. J. Haye, P. M. L. O. Scholte, and F. Tuinstra, Phys. Rev. B **54**, 1557 (1996).

[20] D.-S. Lin, T. Miller, and T. C. Chiang, Phys. Rev. Lett. **67**, 2187 (1991).

[21] P. C. Kelires and J. Tersoff, Phys. Rev. B **63**, 1164 (1989).

[22] L. Pattey, E. L. Bullock, T. Abukawa, S. Kono, and L. S. O. Johansson, Phys. Rev. Lett. **75**, 2538 (1995).

[23] E. Landemark, C. J. Karlsson, Y.-C. Chou, and R. I. G. Uhrberg, Phys. Rev. Lett. **69**, 1588 (1992).

[24] J. E. Rowe and G. K. Wertheim, Phys. Rev. Lett. **69**, 550 (1992); F. L. Himpsel, *ibid.* **69**, 551 (1992); D.-S. Lin, J. A. Carlisle, T. Miller, and T. C. Chiang, *ibid.* **69**, 552 (1992).

[25] X. Yang, R. Cao, J. Terry, and P. Pianetta, Phys. Rev. B **45**, 13 749 (1992).

[26] J. H. Cho, S. Jeong, and M. H. Kang, Phys. Rev. B **50**, 17 139 (1994).

[27] D. E. Jesson, S. J. Pennycook, and J.-M. Baribeau, Phys. Rev. Lett. **66**, 750 (1991).

[28] J. Tersoff, Phys. Rev. B **45**, 8833 (1992).